PHYSICAL REVIEW B **81**, 193203 (2010)

Ab initio study of self-diffusion in silicon over a wide temperature range: Point defect states and migration mechanisms

Shangyi Ma[1,2] and Shaoqing Wang[1]
[1]*Shenyang National Laboratory for Materials Science, Institute of Metal Research, Chinese Academy of Sciences, Shenyang 110016, China*
[2]*Graduate University, Chinese Academy of Sciences, Beijing 100049, China*
(Received 4 April 2010; published 12 May 2010)

We identified the states of intrinsic point defects underlying the self-diffusion in Si and clarified the change of dominant diffusion mechanism responsible for the self-diffusion over a wide temperature range using *ab initio* method. We presented a reliable self-diffusion model that the mechanisms of vacancies and self-interstitials dominate below and above 1220 K, respectively. Our calculations provided a clear picture of Si self-diffusion at lower and higher temperature ascribed to single point defects rather than extended defects. The calculations also provided valuable information on the energy levels and the thermal equilibrium concentrations of point defects, which are highly controversial in experimental reports due to detection limits.

DOI: 10.1103/PhysRevB.81.193203 PACS number(s): 66.30.H−, 61.72.jd, 61.72.jj, 71.15.Mb

The characteristic of self-diffusion in Si remain ambiguous, although it has been established the self-diffusion is predominated by the intrinsic point defects, self-interstitials (I), and vacancies (V). The experimental situation regarding this issue is highly controversial due to detection limits, especially when it comes to the energy levels and equilibrium concentrations of I and V, the specific diffusion states and their migration barriers at cryogenic and elevated temperatures, and the relative contributions of I and V to self-diffusion.[1–6] Though the available computational reports had shined some lights on these topics, large discrepancies exist in various calculations.[2] Thus, the self-diffusion mechanisms in Si are challenged experimentally and theoretically yet.

In this work, we identify the charge states of I and V responsible for the self-diffusion in Si and calculate the self-diffusion coefficients over a wide temperature range. The change of the self-diffusion mechanisms and the crossover temperature of 1220 K are demonstrated.

Under thermal equilibrium conditions, the self-diffusion coefficients $D_{\mathrm{Si}}^{\mathrm{SD}}$ of Si are expressed by[7]

$$D_{\mathrm{Si}}^{\mathrm{SD}} = f_I \sum_q C_{Iq}^{\mathrm{eq}} d_{Iq}/C_0 + f_V \sum_q C_{Vq}^{\mathrm{eq}} d_{Vq}/C_0, \quad (1)$$

where f_I=0.73 and f_V=0.5 are the correlation factors for the diffusion of I and V,[2] $C_{Iq(Vq)}^{\mathrm{eq}}$ and $d_{Iq(Vq)}$ are the equilibrium concentrations and the diffusivities of I (V) in various charge states q ($q=0,\pm1,\pm2$), respectively, and $C_0=5\times10^{22}$ cm^{-3} is Si concentration. From Eq. (1), it is seen $C_{Iq(Vq)}^{\mathrm{eq}}$ and $d_{Iq(Vq)}$ are required to approach the underlying mechanism of Si self-diffusion. Here, the basic calculations are described. The density functional theory (DFT) calculations were performed with Perdew-Burke-Ernzerhof (PBE) version[8] of generalized gradient approximation within plane-wave pseudopotential scheme using QE package.[9] The calculations for I (V) were performed plus (minus) one atom in cubic supercells containing 64, 216, and 512 atoms, using the theoretical lattice constant of 5.475 Å. To circumvent the limits of computational resource, the kinetic cutoffs were set to 30, 20, and 15 Ryd for 64-, 216-, 512-atom models, respectively, and the corresponding energy per atom converges within 0.001, 0.004, and 0.04 eV, respectively. The Brillouin zone was sampled with $2\times2\times2$ **k**-point mesh for 216-atom model and the special **k** point of $\boldsymbol{\Gamma}$ and **L** for 512-atom model. The $2\times2\times2$ mesh was also set for 64-atom model to accord with other highly expensive calculations, e.g., hybrid density functionals and phonon calculations. A neutralizing uniform background charge was introduced for charged defects. The initial configurations were slightly randomized and then relaxed until the atom forces were lower than 3×10^{-4} eV/Å. The calculations are within 0.05 eV errors unless otherwise stated.

Two typical self-interstitials which are expected to be stable in neutral state were considered as starting points for the charged self-interstitials,[10] the displaced hexagonal I_{dh} (Si displacing a little along the direction perpendicular to the plane of the hexagonal Si, C_{3v} symmetry) and the split-⟨110⟩ I_s (Si-Si pair sharing one lattice site in ⟨110⟩ direction, C_{2v} symmetry). Though the starting points might be a restriction, our studies showed our calculations can be comparable well with the establish reports. The relaxation of X^q (I or V with q charge) showed that, I_{dh}^0 relaxed toward tetrahedral site once one hole was trapped, which retained C_{3v} symmetry and nearly degenerated with I_t^{+1} (Si staying at tetrahedral site, T_d symmetry) in energy; I_{dh}^{+1} changed to I_t^{+2} immediately when it caught another hole; I_s^{+1} and I_s^{+2} were saddle points on energy surface and they easily switched to I_{dh}^{+1} and I_t^{+2}, respectively; I_{dh}^{-1}, I_{dh}^{-2}, I_s^{-1}, and I_s^{-2} nearly remained their starting configurations even they caught electrons. For V^q, the charged lattice vacancy V_L^q nearly remained its initial configuration in 64-atom model. Whereas further calculations with larger models indicated that, V_L^{-2} was saddle point and could change to the semivacancy V_S^{-2} (Si situating the center between two neighboring empty lattice sites, 0.15 eV lower in energy than that of V_L^{-2}); V_S^{-1} is almost degenerate with V_L^{-1} in energy. V_S^{-2} and V_S^{-1} are in D_{3d} symmetry. The symmetries of V_L^0, V_L^{+1}, V_L^{+2}, and V_L^{-1} are D_{2d}, D_{2d}, T_d, and C_{2v}, respectively, which consist with the established reports.[11,12]

Once the ground states of X^q were determined, their for-

 ©2010 The American Physical Society

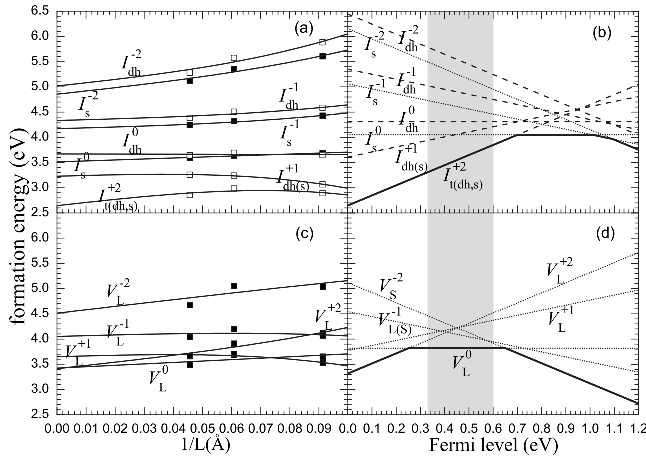

FIG. 1. (a) and (c) show the fitting of formation energies with Makov-Payne scheme in various charge states. (b) and (d) show the formation energies of self-interstitial and vacancies functioned with Fermi level, respectively. The shadow areas indicate the change interval of Fermi level as temperature increases from 0 to 1600 K.

mation energies $E^q_{X_f}$ were computed with the total energies E^q_X by[11] $E^q_{X_f}=E^q_X-N\mu+q(E_{\mathrm{VBM}}+\mu_e)$, where N is the number of Si, μ is Si chemical potential, and μ_e is Fermi level referenced to the valance-band maximum (VBM) E_{VBM} in equivalent bulk. The E_{VBM} position of defect-containing model is different from that of perfect bulk, thus an average potential difference is used to align the VBM of defects.[13] The influence of neutralizing charge was corrected with the Makov-Payne scheme[14]

$$E^{\mathrm{MP}}_{X^q_f}=E^q_{X_f}+q^2\alpha/2L\varepsilon+2\pi qM/3L^3\varepsilon+O(L^{-5}), \qquad (2)$$

where $E^{\mathrm{MP}}_{X^q_f}$ is the formation energy of isolated X^q (or X^q in an infinite sized model), $\alpha=2.8373$ is the Madelung constant for simple cubic, ε is the dielectric constant of Si (we used calculated value 12.8 for consistency), M is the coefficient of L^{-3} term, which can be determined from the fit. Fitted to Eq. (2), $E^{\mathrm{MP}}_{X^q_f}$ was extrapolated, as showed in Figs. 1(a) and 1(c). The formation energy of isolated V_S^{-2} was obtained by correcting the value extrapolated via V_L^{-2} with the energy difference of V_L^{-2} and V_S^{-2} in 216-atom model due to failing to find V_S^{-2} in 64-atom model. The extrapolated values are within 0.1 eV errors for V_L^{+2}, V_L^{-1}, and V_L^{-2}, which may be induced by the lower kinetic cutoffs in 512-atom model and the small 64-atom model which can't afford enough relaxation for vacancies with double charges.

Rinke *et al.* demonstrated the band-gap problem of DFT affects the calculation of self-interstitials formation energy in Si.[15] Alkauskas *et al.* showed the band-gap problem of DFT could be eliminated by tuning the fraction of Hartree-Fock exchange incorporated in hybrid density functionals.[16] Thus, we considered the reliable results can be obtained if one extrapolates the formation energies calculated by tuned hybrid density functionals. Nevertheless, the cost of hybrid density functionals is so high that we hardly afford the calculations with hundreds of atoms. To circumvent the limits, we assumed that the difference of $E^q_{X_f}$ obtained between 64-atom and the extrapolated $E^{\mathrm{MP}}_{X^q_f}$ with DFT-PBE, which is denoted as size-correction term, has the same magnitude as that of calculations with hybrid density functionals. Then the reliable formation energies can be evaluated by correcting the values calculated by hybrid density functionals in 64-atom model with the size-correction terms. The hybrid density functionals which replaces 21% PBE exchange with Hartree-Fock exchange was considered, with which the experimental band gap of 1.2 eV was reproduced. Consequently, the final formation energies $E^{\mathrm{final}}_{X^q_f}$ for X^q were obtained.

The dependences of $E^{\mathrm{final}}_{X^q_f}$ on Fermi level were illustrated in Figs. 1(b) and 1(d). The stable defects were marked by heavy lines. For self-interstitials, $I^{+1}_{dh(s)}$ is unstable and it can be lowered in energy upon capturing a hole instead of raised, in which instance, $I^0_{dh(s)}$, $I^{+1}_{dh(s)}$, and I^{+2}_t are said to form an Anderson negative-U system. The calculations showed I^{+2}_t is predominant in p-type Si, and switch to I^0_s in weak n-type Si, which theoretically confirm the experimental report.[17] Owing to lacking direct experimental evidence, considerable uncertainties exist with respect to the donor and acceptor level for the intrinsic points in p- and n-type Si. In our calculations, the single donor levels are $E_{\mathrm{VBM}}+0.7$ and $E_{\mathrm{VBM}}+0.44$ eV for I_{dh} and I_s, respectively, which fall in the experimental range of 0.17–0.73 eV above VBM.[2] The value of I_s confirms the value of 0.43–0.45 eV above VBM deduced from the formation of radiation defects.[2] Our double donor level is $E_{\mathrm{VBM}}+0.95$ eV for $I_{dh(s)}$ which is comparable well with the rare experimental report of $E_{\mathrm{VBM}}+0.87$ eV.[2] For acceptor levels, the negative-U system is also observed for I^0_{dh}, I^{-1}_{dh}, and I^{-2}_{dh}. The acceptor levels are around $E_{\mathrm{VBM}}+1.03$ eV for I^{-1}_s, I^{-2}_s, I^{-1}_{dh}, and I^{-2}_{dh}. Our single acceptor levels fall in the range of 0.63–1.03 eV above VBM reported by various experiments, and confirm the result of $E_{\mathrm{VBM}}+1.03$ eV suggested by oxidation enhanced diffusion measurements.[2] For vacancies, the characteristic of negative-U can also be noticed for V^0_L, V^{+1}_L, and V^{+2}_L, and for V^0_L, V^{-1}_S, and V^{-2}_S. Our single donor level of $E_{\mathrm{VBM}}+0.05$ eV consists with the direct evidence of $E_{\mathrm{VBM}}+0.05$ eV,[17] whereas the double donor level is 0.3 eV higher than that of measurements (0.11–0.13 eV above VBM). The deviation may be induced by the unrelaxed results in 64-atom model. The acceptor levels of 0.19–1.03 and 0.73–1.13 eV above VBM were reported for single and double acceptor levels, respectively.[2] Our single acceptor level is about $E_{\mathrm{VBM}}+0.73$ eV (with 0.1 eV errors), which confirms the measurements of $E_{\mathrm{VBM}}+0.73$, $E_{\mathrm{VBM}}+0.78$ and $E_{\mathrm{VBM}}+0.68$ eV.[17] Our double acceptor level of $E_{\mathrm{VBM}}+0.58$ eV (with 0.1 eV errors) confirms the value of $E_{\mathrm{VBM}}+0.73$ eV measured by Boyarkina.[2]

The Fermi level of Si always locates around the middle of the band gap. Whereas, the band gap is temperature dependent and it can be described by the empirical expression,[17] $E_{\mathrm{gap}}(T)=E_{\mathrm{gap}}(0)-\alpha T^2/(T+\beta)$, where T is absolute temperature, $E_{\mathrm{gap}}(0)$ is the band gap at 0 K, $\alpha=0.000473$ eV/K and $\beta=636$ K are empirical constants. Hence the Fermi level shifts down from $E_{\mathrm{VBM}}+0.6$ to $E_{\mathrm{VBM}}+0.33$ eV approximately as the temperature increasing from 0 to 1600 K, as illustrated by the shadow areas in Figs. 1(b) and 1(d). One

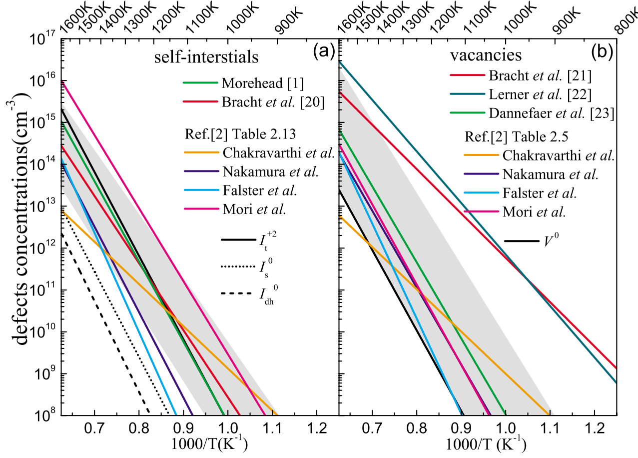

FIG. 2. (Color online) The equilibrium concentration of self-interstitials (a) and vacancies (b). The shadow areas indicate the errors of experimental reports of Bracht *et al.* (for I) and Dannefaer *et al.* (for V).

can notice I_t^{+2} and V_L^0 are the favorable defects in this range, which implies they may be the real ones underlying the self-diffusion in Si. To identify the roles of I_t^{+2} and V_L^0 in self-diffusion, we focused our attention on their thermal equilibrium concentrations and diffusivities in the following calculations.

It is known the thermal equilibrium concentration of neutral defect X^0 can be expressed as[1] $C_{X^0}^{\text{eq}} = \theta_{X^0} C_0 \exp[-F_{X^0}^f/(kT)]$, where θ_{X^0} is the degree of internal freedom for X^0, $F_{X^0}^f$ is the formation free energy of X^0 and it is summed from the $E_{X_f^q}^{\text{final}}$ and the vibration formation energy $\Delta F_{X^0}^f$. The $\Delta F_{X^0}^f$ is calculated with $\Delta F_{X^0}^f = F_{X^0}^{\text{vib}} - (N \pm 1) F_{\text{bulk}}^{\text{vib}}/N$, where N is the number of Si in bulk model, and $F_{X^0(\text{bulk})}^{\text{vib}}$ is the vibrational free energy of X^0 (bulk). The vibrational free energy of a model containing N atoms was calculated with phonon density of states (PDOS) $g(\omega)$ using harmonic approximation $F^{vib} = 3NkT\int_0^\infty \ln[2\sinh(\hbar\omega/2kT)]g(\omega)d\omega$. The PDOS was calculated with density functional perturbation theory[18] using 64-atom model. Our tests showed the methods confirmed the calculations within 2% errors. More details about the tests can be found in Ref. 19. Using the internal freedom of 4 for I_{dh}^0, 6 for I_s^0, and 3 for V_L^0,[10] we estimated their concentrations and illustrated them in Fig. 2. For I_t^{+2}, its concentration was obtained by the expression[17]

$$C_{I^{+2}}^{\text{eq}} = C_{I^0}^{\text{eq}}(\theta_{I_t^{+2}}/\theta_{I^0})\exp[-(2E_{\text{fermi}} - E_{I^{+2}}^{(+2/1)} - E_{I^{+1}}^{(+1/0)})/kT], \tag{3}$$

where $\theta_{I_t^{+2}}$ and θ_{I^0}, respectively, denote the degeneracy factors of I_t^{+1} and I^0, and $\theta_{I_t^{+2}} = \theta_{I^0}$ in this instance, $E_{I^{+1}}^{(+1/0)}$ and $E_{I^{+2}}^{(+2/1)}$ are the single and double donor levels reference to VBM. We evaluated the concentration of I_t^{+2} and showed it in Fig. 2(a), in which some selected experiments[2,20–23] were also given for comparison. It is showed the concentration of $I_{dh(s)}^0$ is negligible compared with that of I_t^{+2}. The calculated concentration of I_t^{+2} is comparable with most experiments within one order of magnitude, especially agree well with the estimation of Morehead.[1] It can be fitted in the form of $C_I^{\text{eq}} = 7.5 \times 10^{27} \exp[-(3.98 \pm 0.07)/(kT)]$ cm^{-3} approximately. For V_L^0, it can also be fitted in the form of $C_V^{\text{eq}} = 2.47 \times 10^{25} \exp[-(3.81 \pm 0.06)/(kT)]$ cm^{-3}, which is about one order of magnitude lower than that of most estimations.

As the last unknown quantity in Eq. (1), d_{Xq} can be obtained with the jump length r, the number of possible neighboring jump site z, and the jump rate Γ related with jump event, $d_{Xq} = (z/6)r^2\Gamma$.[7] According to the harmonic transition state theory, the jump rate Γ is written in terms of migration barrier ΔE_m and effective frequency v^*, $\Gamma = v^* \exp(-\Delta E_m/kT)$, where v^* is the ratio of the product of the N normal frequencies v_j of the system at the initial point to the $N-1$ normal frequencies v_j' at the saddle point, $v^* = (\Pi_j^N v_j)/(\Pi_j^{N-1} v_j')$.[24] The normal frequencies were also calculated with the same scheme of PDOS. Two probable diffusion paths for I_t^{+2} were identified via climbing image nudged elastic band method.[25] In path I, I_t^{+2} migrated to neighboring tetrahedral site via the saddle point I_{ih}^{+2} (Si situating at the center of hexagonal ring) under the interstitials mechanism, $I_t^{+2} \to I_{ih}^{+2} \to I_t^{+2}$, with 1.15 eV barrier. Whereas I_t^{+2} migrated under the "kick-out" mechanism in path II, $I_t^{+2} \to I_s^{+2} \to I_t^{+2}$, in which I_t^{+2} approached to lattice site and formed I_s^{+2} and then occupied the site by "kicking-out" the original Si to tetrahedral site, with 1.20 eV barrier. The parameters for evaluating the diffusivity were $z=4$, $r=2.40$ Å, and $\Gamma = 1.79\text{E}14$ s^{-1} for path I, and $z=4$, $r=4.6$ Å, and $\Gamma = 1.96\text{E}14$ s^{-1} for path II. Consequently, the respective diffusivity was obtained, $d_I^{t^{+2}} = 0.069 \exp[-(1.15 \pm 0.02)/(kT)]$ cm^2 s^{-1} for path I and $d_{II}^{t^{+2}} = 0.276 \exp[-(1.20 \pm 0.02)/(kT)]$ cm^2 s^{-1} for path II. Considered the jump event taking place only along one of the two paths per time, the contribution weight of each path is required. Since Voter had demonstrated that the average time τ for jump event is in inverse proportion to its jump rate,[26] one can deduce that the average number of jump event occurring along specific path is in direct proportion to its jump rate. Thus, we evaluated and normalized the contribution weights of path I and II by their jump rates. Finally, the effective diffusivity of I_t^{+2} was obtained in the form of $d_{I_t^{+2}} = 0.17 \exp[-(1.20 \pm 0.02)/(kT)]$ cm^2 s^{-1} by fitting the sum of weighted $d_I^{t^{+2}}$ and $d_{II}^{t^{+2}}$. For vacancy, V_L^0 migrated to the nearest site by overcoming 0.28 eV barriers, which was comparable with the value of 0.45 ± 0.02 eV measured at cryogenic temperature.[6] The diffusivity of V_L^0 was also obtained with the parameters $z=4$, $r=1.79$ Å, and $\Gamma = 1.08\text{E}13$ s^{-1}, $d_{V^0} = 0.0023 \exp[-(0.28 \pm 0.04)/(kT)]$ cm^2 s^{-1}. Our calculated diffusivity of vacancy consisted well with the experimental report, $d_{V^0} = 0.0012 \exp[-(0.45 \pm 0.02)/(kT)]$ cm^2 s^{-1},[6] especially our prefactor agreeing within a factor of 2. This good agreement validated the methods used. Combining the concentrations and diffusivities of the candidates, I_t^{+2} for self-interstitials and V^0 for vacancies, and their correlation factors, we evaluated the diffusion coefficients of I_t^{+2} and V_L^0 in the form of, $D_{I_t^{+2}} = 1.862 \times 10^4 \exp[-(5.18 \pm 0.09)/(kT)]$ cm^2 s^{-1} and $D_{V^0} = 0.568 \exp[-(4.09 \pm 0.1)/(kT)]$

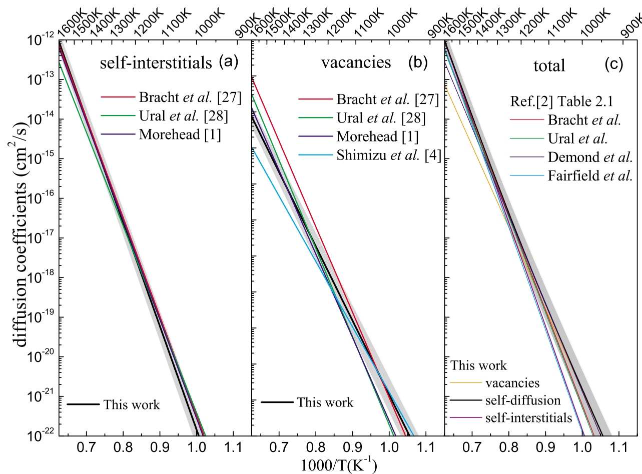

FIG. 3. (Color online) The calculated and measured self-diffusion coefficients in Si: (a) self-interstitials, (b) vacancies, and (c) the sum of self-interstitials and vacancies. The shadow areas indicate the errors of the calculations.

$cm^2\ s^{-1}$, respectively, which were showed in Figs. 3(a) and 3(b). The calculations of self-interstitials consist with the values measured by Morehead,[1] Bracht *et al.*,[27] and Ural *et al.*[28] For self-interstitials, only the contributions of I_t^{+2} were considered, and the contributions from other states were ignored due to their negligible effects at higher temperatures. However, their contributions are comparable with that of I_t^{+2} at lower temperature; it may be the reason why some small deviations exist compared with experiments at lower temperatures. For vacancies, the calculations are comparable well with the measurements by Morehead,[1] Shimizu *et al.*,[4] Bracht *et al.*,[27] and Ural *et al.*[28] Using single vacancy model, we obtained the diffusion coefficients of vacancy consistent with experiments, which theoretically confirm the conclusion deduced by Watkins that the diffusion properties of vacancies are identical at elevated and cryogenic temperatures.[6] Based on the comparison of the calculations and experiments, one may infer I_t^{+2} and V^0 are the real ones mainly responsible for the results of self-interstitials and vacancies measured by experiments, respectively.

Summing the individual contributions of self-interstitials and vacancies, we evaluated the self-diffusion coefficients of Si in the form of $D_{Si}^{SD}=1.862\times 10^4 \exp[-(5.18\pm 0.09)/(kT)]+0.568 \exp[-(4.09\pm 0.1)/(kT)]$ $cm^2\ s^{-1}$. It is seen in Fig. 3(c) that the calculations agree well with experiments performed by Bracht *et al.*, Ural *et al.*, Demond *et al.*, and Fairfield *et al.* using various isotope of Si as tracer.[2] The good agreements further confirm that I_t^{+2} and V^0 are the diffusion species underlying the self-diffusion in Si. The individual diffusion contributions of self-interstitials and vacancies are showed. One can see vacancies dominate the self-diffusion at low temperatures, while self-interstitials play a dominant role at higher temperatures. Their intersection situates approximately at 1220 K, which is about 50 K higher than the crossover temperatures reported by Shimizu *et al.*[4] Thus, the break point in the diffusion coefficients showing non-Arrhenius behavior exists at 1220 K. The calculations imply that Si self-diffusion has activation energy of about 5.18 and 4.09 eV for temperatures greater and less than 1220 K, respectively, due to the changing of dominant role responsible self-diffusion.

This work was supported by the National Basic Research Program of China (Grant No. 2006CB605103).

[1] P. M. Fahey *et al.*, Rev. Mod. Phys. **61**, 289 (1989).
[2] P. Pichler, *Intrinsic Point Defects, Impurities, and Their Diffusion in Silicon* (Springer-Verlag, Wien, New York, 2004).
[3] D. Caliste and P. Pochet, Phys. Rev. Lett. **97**, 135901 (2006).
[4] Y. Shimizu *et al.*, Phys. Rev. Lett. **98**, 095901 (2007).
[5] R. Vaidyanathan *et al.*, Phys. Rev. B **75**, 195209 (2007).
[6] G. D. Watkins, J. Appl. Phys. **103**, 106106 (2008).
[7] T. Y. Tan *et al.*, in *Diffusion in Condensed Matter*, edited by P. Heitjans and J. Karger (Springer-Verlag, Berlin, Heidelberg, 2005).
[8] J. P. Perdew *et al.*, Phys. Rev. Lett. **77**, 3865 (1996).
[9] P. Giannozzi *et al.*, J. Phys.: Condens. Matter **21**, 395502 (2009).
[10] O. K. Al-Mushadani and R. J. Needs, Phys. Rev. B **68**, 235205 (2003).
[11] D. A. Drabold *et al.*, *Theory of Defects in Semiconductors* (Springer-Verlag, Berlin, Heidelberg, 2007).
[12] A. F. Wright and N. A. Modine, Phys. Rev. B **74**, 235209 (2006).
[13] T. Mattila and A. Zunger, Phys. Rev. B **58**, 1367 (1998).
[14] G. Makov and M. C. Payne, Phys. Rev. B **51**, 4014 (1995).
[15] P. Rinke *et al.*, Phys. Rev. Lett. **102**, 026402 (2009).
[16] A. Alkauskas *et al.*, Phys. Rev. Lett. **101**, 106802 (2008).
[17] E. G. Seebauer *et al.*, *Charged Semiconductor Defects* (Springer-Verlag, London, 2009).
[18] S. Baroni *et al.*, Rev. Mod. Phys. **73**, 515 (2001).
[19] S. Y. Ma and S.-Q. Wang, Eur. Phys. J. B **72**, 567 (2009).
[20] H. Bracht *et al.*, Phys. Rev. B **52**, 16542 (1995).
[21] H. Bracht *et al.*, Phys. Rev. Lett. **91**, 245502 (2003).
[22] L. Lerner and N. A. Stolwijk, Appl. Phys. Lett. **86**, 011901 (2005).
[23] S. Dannefaer *et al.*, Phys. Rev. Lett. **56**, 2195 (1986).
[24] G. H. Vineyard, J. Phys. Chem. Solids **3**, 121 (1957).
[25] G. Henkelman *et al.*, J. Chem. Phys. **113**, 9901 (2000).
[26] K. E. Sickafus *et al.*, *Radiation Effects in Solids* (Springer, Netherlands, 2007).
[27] H. Bracht *et al.*, Phys. Rev. B **75**, 035211 (2007).
[28] A. Ural *et al.*, Phys. Rev. Lett. **83**, 3454 (1999).